

Impacts of Shunt Reactors on Transmission Line Protection

Eithar Nashawati
Oncor Electric Delivery

Normann Fischer, Bin Le, and Douglas Taylor
Schweitzer Engineering Laboratories, Inc.

Revised edition released November 2013

Originally presented at the
38th Annual Western Protective Relay Conference, October 2011

Impacts of Shunt Reactors on Transmission Line Protection

Eithar Nashawati, *Oncor Electric Delivery*

Normann Fischer, Bin Le, and Douglas Taylor, *Schweitzer Engineering Laboratories, Inc.*

Abstract—Shunt reactors are installed to offset the capacitive effect of transmission lines and therefore improve the voltage profiles of transmission lines. In addition, they also help regulate the volt/VAR of power systems. Specific implementations of shunt reactors may greatly differ between utilities. Reactors can be placed on a section of the transmission line or on the adjacent bus. Current transformers (CTs) may be installed on the reactors, or the line protection devices may rely on bus CTs. Each philosophy presents challenges for reactor, line, and/or bus protection schemes.

This paper examines typical implementations for shunt reactors, considers their advantages and disadvantages, and presents protection requirements and solutions required by each implementation. For example, a line-installed reactor can be kept within the line protection zone or taken out of the line protection zone by measuring its current and effectively subtracting it from the total line current. In the former case, the reactor represents a shunt branch within the zone with the possibility of inrush current, effect of zero-sequence feed into the zone during external ground faults, and so on. In the latter case, we need to consider the performance of reactor CTs during inrush conditions and ground faults forcing the zero-sequence fault current in the reactor and the potential impact of CT errors or CT saturation on the security of line protection, especially if sensitive protection elements are used.

We begin the paper by examining why shunt reactors are used on power lines and then discuss how to calculate the size of the reactors. Next, we see what impact these shunt reactors have on the power system. Lastly, we investigate the impact shunt reactors have on line protection schemes.

I. INTRODUCTION

For the purposes of accurate modeling, transmission lines are generally categorized into the following three types with regard to their physical length [1]:

- Short lines (less than 50 miles).
- Medium-length lines (greater than 50 miles but less than 120 miles).
- Long lines (greater than 120 miles).

The equivalent transmission line model changes based on the physical line length; accordingly, for a short line, we only consider the series parameters and ignore the shunt parameters, as shown in Fig. 1.

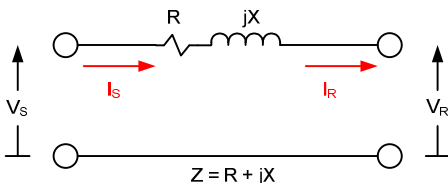


Fig. 1. Model used to represent a short transmission line

For short lines, the sending-end voltage (V_S) and current (I_S) are calculated as follows (in the following equations, all variables are complex numbers—phasors and impedances—unless indicated otherwise):

$$\begin{aligned} V_S &= V_R + ZI_R \\ I_S &= I_R \end{aligned} \quad (1)$$

where:

Z is the line impedance.

V_R is the receiving-end voltage.

I_R is the receiving-end current.

For medium-length lines, the parasitic capacitance of the line becomes significant enough that it impacts the sending-end and receiving-end voltages and currents; therefore, it is included as shunt components in the equivalent line model. The equivalent π circuit, as shown in Fig. 2, is generally used when modeling medium-length transmission lines.

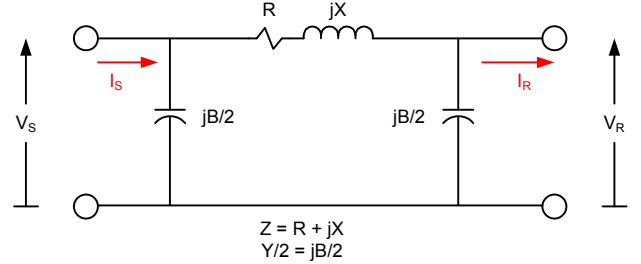


Fig. 2. Equivalent π circuit representing a medium-length transmission line

For the medium-length line model, the sending-end voltage and current are calculated as follows:

$$\begin{aligned} V_S &= \left(1 + \frac{ZY}{2}\right) \cdot V_R + ZI_R \\ I_S &= Y \left(1 + \frac{ZY}{4}\right) \cdot V_R + \left(1 + \frac{ZY}{2}\right) \cdot I_R \end{aligned} \quad (2)$$

where:

Y is the line admittance.

Equation (2) is often expressed in matrix form; this is the form commonly found in most reference material and textbooks:

$$\begin{bmatrix} V_S \\ I_S \end{bmatrix} = \begin{bmatrix} A & B \\ C & D \end{bmatrix} \cdot \begin{bmatrix} V_R \\ I_R \end{bmatrix} \quad (3)$$

where:

$$A = D = \left(1 + \frac{ZY}{2}\right)$$

$$B = Z$$

$$C = Y \left(1 + \frac{ZY}{4}\right)$$

In long lines, the distributed effects of the parameters become significant, and the line must be represented by the equivalent π circuit. Alternatively, the line may be represented by smaller cascaded sections, where each section is represented by an equivalent π circuit, similar to the one used for a medium-length line. For the purpose of this paper, we consider a long line as being composed of multiple sections of equivalent π circuits, as shown in Fig. 3.

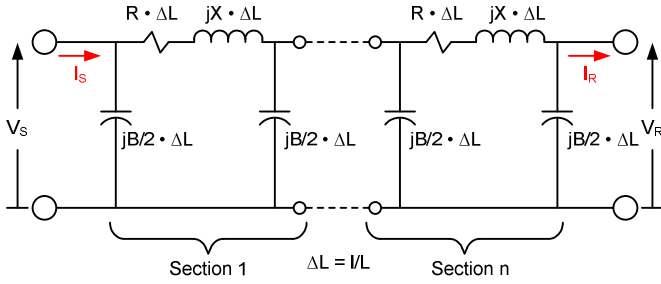


Fig. 3. Multiple equivalent π circuits used to represent a long transmission line

In Fig. 3, ΔL is the per-unit (pu) section length defined as the ratio of the incremental line section l to the total line length L (both given in the same unit of length). The sending-end voltage and current for a long line composed of n equivalent π sections are determined as follows, with $n = L/l$. Calculate the incremental sending-end voltage and current for Section n using (4). The sending-end voltage of Section n then becomes the receiving-end voltage and current for Section $n - 1$. The process is repeated until the final sending-end voltage and current are obtained.

$$\begin{bmatrix} V_{S(n)} \\ I_{S(n)} \end{bmatrix} = \Delta L \cdot \begin{bmatrix} A & B \\ C & D \end{bmatrix} \cdot \begin{bmatrix} V_{R(n)} \\ I_{R(n)} \end{bmatrix} \quad (4)$$

where:

ΔL is l/L (pu line section).

l is the incremental line section length.

L is the total line length.

Examining (1) representing the short line, we can make the following observations:

- The sending-end voltage (V_S) is dependent only on the series voltage drop (load current) and the receiving-end voltage (V_R).
- The sending-end voltage will always be greater than or equal to the receiving voltage (V_R), unless the load is capacitive.

For medium-length and long lines, we can make the following observations:

- The sending-end voltage is dependent on the receiving-end voltage and the series voltage drop, but the series voltage drop is dependent not solely on the load current but also on the current being drawn by the parasitic capacitance of the line (charging current of the line).
- The receiving-end voltage can be higher than the sending-end voltage if the charging current is predominant.

From these observations, we see that for short lines, we can basically ignore the impact of capacitive current from a voltage regulation point of view. Medium-length and long lines, on the other hand, can have voltages at their receiving ends much higher than at the sending end, and this can create issues such as overfluxing of power transformers and overstressing of line insulators. But before we can come up with a solution for this problem, it is important to understand what causes this overvoltage.

Examine the medium-length line equivalent circuit in Fig. 2. Notice that the circuit has both a VAR source (the shunt capacitor) and a VAR sink (the series line impedance). The VARs produced by the line are determined by the sending-end voltage (V_S) and the line susceptance (B). Because the line susceptance is fixed and the sending-end voltage is relatively constant, the VARs produced by a transmission line are relatively constant.

$$Q_{\text{Produced}} = |V_S|^2 B \quad (5)$$

The VARs sunk (consumed) on the line are dependent on the line reactance (X) and the line current (I_L). We know that the line impedance is fixed but the load current can vary from zero to full load or even temporary overload given the thermal constraints for the given line. This means the VARs consumed by the line are directly dependent on the load current.

$$Q_{\text{Consumed}} = |I_L|^2 X \quad (6)$$

$$I_L = \left(I_S - j \cdot \frac{V_S B}{2} \right)$$

The result of this is that under light-load conditions, the line produces more VARs than it consumes; therefore, there is an excess of VARs on the line, resulting in the receiving-end voltage being higher than the sending-end voltage. In order to consume the excess VARs when the system is lightly loaded, a device that absorbs VARs must be added to the system. This

addition should be done in the vicinity of the line to minimize the losses caused by the reactive current. Because we know that inductors absorb VARs, a reactor is connected in parallel with the shunt capacitance of the line. Therefore, the VARs produced by the shunt capacitance of the line (Q_{GEN}) are consumed by the shunt reactors connected in parallel with the line (Q_{SINK}), as shown in Fig. 4.

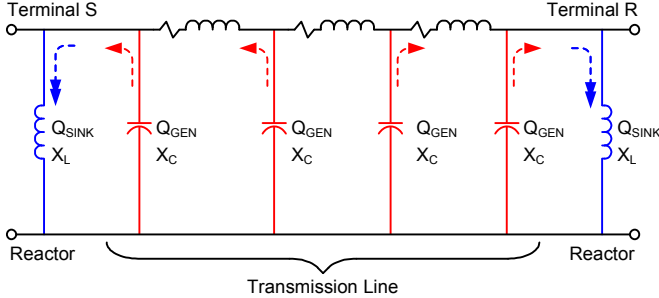


Fig. 4. VARs created by the parasitic capacitance of the line are absorbed by shunt reactors

The value of the shunt reactor to be connected to the line is discussed in detail in Section II.

II. DETERMINING THE VAR RATING OF A SHUNT REACTOR

A. General Discussion

Extra-high-voltage (EHV) transmission lines are employed to transmit power over vast distances; due to the long lengths, these lines have large shunt capacitances associated with them. Shunt capacitance exists between the individual phases of the transmission line and also between the phase conductors and ground. When a transmission line is energized, it draws a large charging current because of the large shunt capacitance of the line. This current is mainly capacitive, and as we see from (2), the voltage at the receiving end of the line can become greater than the voltage at the sending end. To avoid an overvoltage condition along the line and the possibility of damaging the line insulator, shunt reactors are installed at the terminals of the line. As shown in Section III, this brings the voltage levels along the line to within specified levels.

The degree of compensation of a line determines the size and configuration of the reactor scheme. Perfect compensation (100 percent) is not always the best choice, even though this results in a flat voltage profile along the line under no-load conditions. A perfectly tuned reactor will need to be switched out of service well before the line reaches its rated full-load current, in order to maintain the voltage regulation at the receiving end of the line.

B. Three-Pole Protection Tripping Applications

Common practice is for the reactors to compensate between 70 and 80 percent of the line shunt capacitance, which allows the reactors to remain in service when the line is moderately loaded. The reactor only needs to be taken out of service when the line is heavily loaded in order to maintain the voltage within the prescribed limits [2]. For the purpose of this paper, a four-reactor scheme as shown in Fig. 5 is selected. The fourth reactor, X_n , is only needed in single-pole tripping applications, as discussed in Section II, Subsection C.

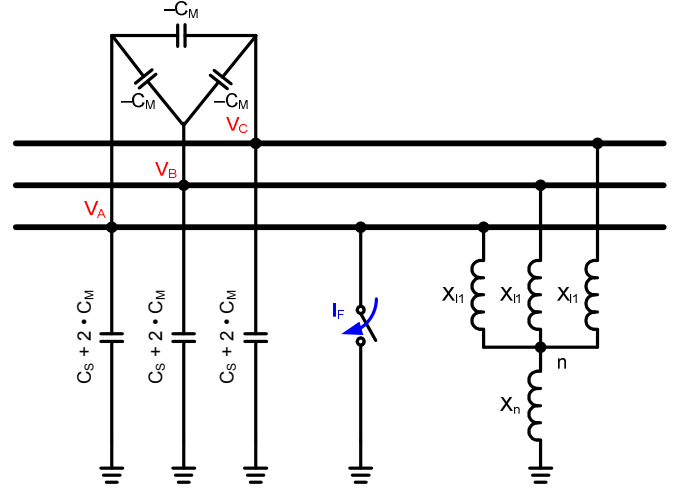


Fig. 5. Connection scheme with four reactor units

The four-reactor scheme reduces the installation cost by using the minimum number of reactor tanks, because the per-kilovar cost decreases with the increase in the unit size [3]. If we know the positive-sequence susceptance (B_{1L}) of the line and the percent of compensation (η), we can calculate the impedance of the phase-to-neutral reactance or positive-sequence reactance (X_{11}) using:

$$X_{11} = \frac{1}{(\eta \cdot B_{1L})} \quad (7)$$

Assuming that reactors are deployed at both line terminals, the VAR rating of a single line reactor unit can be calculated using the rated line-to-neutral voltage V_{LN} and the positive-sequence reactance as follows:

$$S_{1\phi} = \frac{|V_{LN}|^2}{2 \cdot X_{11}} \quad (8)$$

A further consideration is whether to install the reactors on the line or the bus. Should the reactor be connected on the bus, multiple lines benefit from the reactor, which further lowers the capital investment. Under normal system operation conditions, transmission lines are switched in and out of service; therefore, the amount of reactive current compensation being supplied by the reactor varies. The size of the bus reactor has to be such that it provides compensation for the system with all the feeders in service. A properly sized earthing switch is required for each feeder for the safety of maintenance personnel [4]. After the line breaker trips, the motor-operated earthing switch needs to be closed to discharge the energy trapped on the line. The travel time of its moving contact is long, and arcing will persist, once formed, until the switch is physically closed. On the other hand, if the reactor is connected to the line, the compensation is fixed and there is almost no stress on the earthing switch when it operates to ground the power line. However, when a line is de-energized, the system will experience a subsynchronous ringdown due to the interaction of the reactor and the line capacitance.

C. Single-Pole Protection Tripping Applications

Single-pole tripping and reclosing for single-line-to-ground faults help improve system stability and prevent unnecessary separation of the interconnected power system. Single-pole tripping is often employed at the transmission level, but long EHV line applications often experience difficulty in successfully clearing single-phase faults when only de-energizing the faulted phase. When the faulted phase breaker poles are open, the primary circuit stops supplying current to the fault directly through the faulted conductor. But because of the capacitive coupling between the faulted phase and the two remaining healthy phases, capacitive current flows between the unfaulted phases and the faulted phase, effectively supplying a fault current and preventing the arc from extinguishing. Once the primary arc has been established, the current required to maintain the arc is low enough to be maintained by the capacitive current flowing from the unfaulted phases to the faulted phase. This phenomenon is known as secondary arcing [3]. If reclosing occurs before the secondary arc is extinguished, it is no different than reclosing back into a permanent fault.

To extinguish the secondary arc (neutralize the secondary arcing current), a fourth reactor, the neutral reactor, is installed between the phase reactor neutral point and ground (Fig. 5). The charging current for a transmission line is determined by multiplying the capacitance matrix with the voltage matrix:

$$\begin{bmatrix} I_{Ac} \\ I_{Bc} \\ I_{Cc} \end{bmatrix} = j\omega \cdot \begin{bmatrix} C_S & C_M & C_M \\ C_M & C_S & C_M \\ C_M & C_M & C_S \end{bmatrix} \cdot \begin{bmatrix} V_A \\ V_B \\ V_C \end{bmatrix} \quad (9)$$

where:

C_S is the self-capacitance of the line.

C_M is the mutual capacitance of the line.

Assume that the A-phase is the faulted phase and that the A-phase breakers have been opened at both ends of the line. Using (9), we can calculate the A-phase capacitive current being supplied by the two remaining healthy phases as follows:

$$I_{Ac} = j \cdot \omega C_M \cdot (V_B + V_C) \quad (10)$$

From (10), we see that the magnitude of the coupling current is proportional to the mutual capacitance between the phases. Because long EHV transmission lines have a high mutual capacitance, single-pole tripping is not often successful under these conditions.

With the addition of a neutral reactor, the goal is to create an LC resonance circuit so that the paralleled circuit between phase conductors has an infinitely large impedance when viewed externally. In other words, the interphase inductive current supplied from the shunt reactor configuration should have the same magnitude as the capacitive current but with

opposite polarity. The equivalent shunt reactor current with respect to phase voltage is given by:

$$\begin{bmatrix} I_{A1} \\ I_{B1} \\ I_{C1} \end{bmatrix} = -j \cdot A \begin{bmatrix} X_{10}^{-1} & 0 & 0 \\ 0 & X_{11}^{-1} & 0 \\ 0 & 0 & X_{12}^{-1} \end{bmatrix} \cdot A^{-1} \cdot \begin{bmatrix} V_A \\ V_B \\ V_C \end{bmatrix} \quad (11)$$

where:

$$A = \begin{bmatrix} 1 & 1 & 1 \\ 1 & a^2 & a \\ 1 & a & a^2 \end{bmatrix}$$

$$a = 1 \angle 120^\circ$$

$X_{11}^{-1} = X_{12}^{-1}$, the inverse of the positive-sequence shunt reactor impedance.

$X_{10}^{-1} = (X_{11} + 3 \cdot X_n)^{-1}$, the inverse of the zero-sequence shunt reactor impedance.

Solving (11), we obtain the following result for the shunt reactor current:

$$\begin{bmatrix} I_{A1} \\ I_{B1} \\ I_{C1} \end{bmatrix} = -j \cdot \begin{bmatrix} \alpha_s & \beta_M & \beta_M \\ \beta_M & \alpha_s & \beta_M \\ \beta_M & \beta_M & \alpha_s \end{bmatrix} \cdot \begin{bmatrix} V_A \\ V_B \\ V_C \end{bmatrix} \quad (12)$$

where:

$$\alpha_s = (X_{10}^{-1} + 2 \cdot X_{11}^{-1})/3$$

$$\beta_M = (X_{10}^{-1} - X_{11}^{-1})/3$$

For the A-phase fault case, the A-phase inductive current drawn by the line reactors is:

$$I_{A1} = -j \cdot \beta_M \cdot (V_B + V_C) \quad (13)$$

To satisfy the need of having $\overline{I_{A1}} + \overline{I_{Ac}} = 0$, it is clear by comparing (10) and (13) that the mutual inductive susceptance $(X_{10}^{-1} - X_{11}^{-1})/3$ must match the mutual capacitive susceptance ωC_M . This concept is graphically illustrated in Fig. 6.

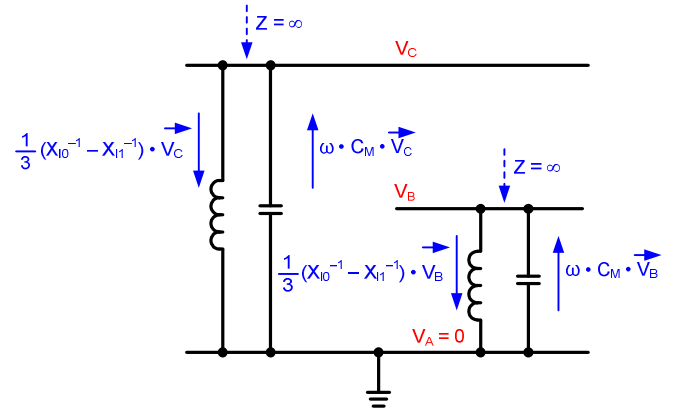


Fig. 6. Interphase LC resonance circuit

We know that the mutual capacitance (C_M) is one-third of the difference between the zero-sequence (C_0) and positive-sequence (C_1) capacitances, which are known line parameters. The result of solving those equations is the required impedance of the neutral reactor:

$$X_n = \frac{1}{3} \cdot \left\{ \left[\omega \cdot (C_0 - C_1) + \frac{1}{X_{ll}} \right]^{-1} - X_{ll} \right\} \quad (14)$$

If the reactor neutral point is directly grounded, the wye-connected reactor group has identical positive-, negative-, and zero-sequence impedances. Effectively, the mutual inductive susceptance between the phases does not exist, and there is no neutralization of capacitive current.

The appendix includes the circuit diagram and details of a model power system implemented in a Real Time Digital Simulator (RTDS[®]). We used this model to validate the equations presented in this paper and to obtain the transient and steady-state waveforms that are presented throughout this paper. We refer to this power system model as the test system.

Using (10), we calculate the capacitance current supplied by the B-phase and C-phase for an A-phase fault during a single-pole open condition for the test system as 84 A_{rms} (120 A_{peak}). Comparing this calculated value with the secondary arcing current without neutralization (blue trace) from Fig. 7, we see that the values agree with one another. Fig. 7 also includes the fault current flowing to ground when the proper neutral reactor is installed (red trace). Note that the magnitude of the fault current is low enough for the arc to self-extinguish.

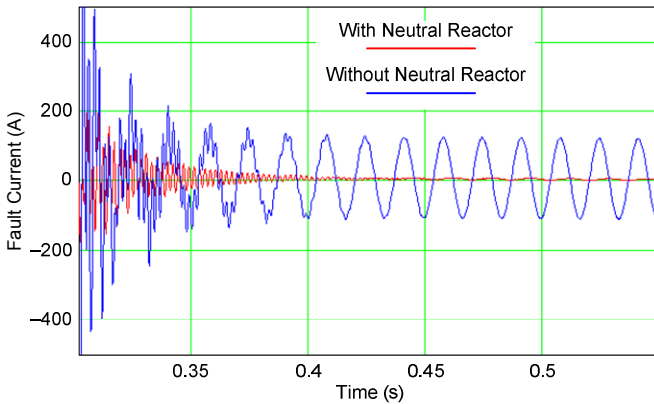


Fig. 7. Comparison of secondary arcing current with and without neutral reactor

Using (14), we calculate the impedance (X_n) or inductance (L_n) of the neutral reactor rather than its VAR rating. The neutral reactor only comes into play when a single-line-to-ground fault occurs on the system. With the A-phase experiencing a fault and the other two phases healthy, the voltage at the neutral of reactor bank (V_n) is:

$$V_n = \left| \frac{(V_B + V_C)}{3 + (X_{ll}/X_n)} \right| = \left| \frac{V_{LN}}{3 + (X_{ll}/X_n)} \right| \quad (15)$$

Using the calculated neutral-to-ground voltage (V_n), we can determine the short-time VAR rating of the neutral reactor. Assuming that grounding reactors are installed at both substations, the VAR rating for the reactor at one substation can be calculated as follows:

$$S_n = \frac{|V_n|^2}{2 \cdot X_n} \quad (16)$$

Note that the reactor does not need to be rated for continuous operation at this calculated reactive power level. The reactor needs to be rated such that it is capable of dissipating the heat during the fault-clearing time plus the pole open time. Prior to the breaker operating, the A-phase voltage usually does not collapse to zero at the reactor location (except in the case of a fault being close in to the terminal). This lowers the fault-time VAR rating of the reactor further. During the pole open period, all the energy stored in the faulted phase is dissipated into the earth, thereby bringing the faulted phase potential close to zero or ground potential. The rating of the neutral reactor (S_n) is a good indication of how fast the reactor absorbs VARs during the pole open period while the arc is being extinguished. Because the pole open period is much longer than the fault-clearing time, S_n multiplied by the pole open time should be used to calculate the amount of energy dissipated in the neutral reactor.

III. EFFECTS OF A SHUNT REACTOR ON THE POWER SYSTEM

Shunt reactors amplify and introduce numerous behaviors in the power system that would otherwise go unnoticed or be nonexistent. This section deals with several of these behaviors, organized into two categories: normal system operation and faulted system operation.

A. Normal Power System Operation

1) Reactor Energization

Any device that has magnetic material in its construction is prone to inrush currents during device energization. Shunt reactors are either designed with air cores or with magnetic cores with intentional air gaps. The purpose of both of these designs is to increase the linearity of the device inductance, which helps to reduce the harmonic content that the reactor injects back into the power system. A reactor built with an air core cannot saturate and thus is not prone to magnetizing inrush current. However, magnetic-core reactors, which are found almost exclusively on EHV lines because of their superior energy density, often draw a slightly distorted sinusoidal current but with a significant dc component [5]. The slight distortion found in reactor inrush current is quite unlike a power transformer inrush current, which is rich in second and fourth harmonics.

The level of the dc component is most influenced by the point of the voltage waveform at which the reactor is energized—a voltage zero crossing causing the worst offset. This dc offset often takes several seconds to decay because of the low losses exhibited by the reactor (high X/R ratio) and can cause saturation of current transformers (CTs), as well as saturation of local power transformers [6]. Because the

different phases of a saturated inductor draw unbalanced inrush current in the three phases, the neutral carries zero-sequence current that might cause issues for zero-sequence protection elements.

The reactor inrush current is only slightly distorted—even when there is significant dc offset—because of the magnetic characteristics of the device. Shunt reactor magnetizing curves are designed with a knee point around 1.25 pu of the operating voltage, which is considerably higher than the knee point of a transformer, generally around 1.1 pu [2]. The shunt reactor has a greater operating range in the linear region compared with that of a transformer. More importantly, the gaps introduced in the reactor core mean that the change in slope of the magnetizing curve past the knee point of the core is much less dramatic than that of a transformer. Even when the reactor core is operating in saturation, the gentler slope draws significantly less harmonic content compared with a power transformer.

Fig. 8 is a plot of the inrush current resulting from the energizing of a line reactor installed in the test system described in the appendix. In the simulation, the reactor was energized at a voltage zero crossing. Notice from the plot how, unlike with transformer inrush current, the reactor inrush current is fairly sinusoidal but contains a significant dc offset.

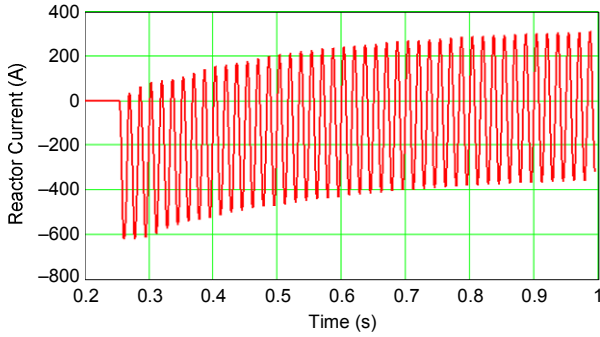


Fig. 8. Shunt reactor inrush current when energized at voltage zero

An obvious but important point to mention is that shunt reactors installed on the bus stay energized so long as the bus is energized and are not subjected to inrush currents when lines are switched in or out.

2) Overvoltage of Shunt Reactors

While overvoltage conditions can cause power transformers to draw elevated third- and fifth-harmonic currents, shunt reactors are rather immune to such operating conditions for the design reasons already mentioned. Because the knee point of the reactor is around 1.25 pu of the nominal voltage, there is significant room for voltage increase before the reactor core saturates. Additionally, if an overvoltage condition does cause core saturation, the third- and fifth-harmonic current content is limited because of the air gaps in the reactor core.

3) Shunt Reactors and System Loading Effects on the Voltage Profile

We have already mentioned that when a line is lightly loaded, the VARs supplied to the power system exceed the VARs consumed, which leads to elevated voltage levels

throughout the transmission line. This behavior is easily shown by examining (2). Here, we see that under no-load conditions (i.e., the breaker at the receiving end is open), the receiving-end current is zero and the ratio of the receiving-end voltage to the sending-end voltage is $1/A$, where A has been defined under (3).

A distributed line model was used for the transmission line of the test system described. The positive-sequence line impedance and shunt capacitance for this line are as follows:

$$\begin{aligned} Z_1 &= 107.68 \angle 87.33^\circ \Omega \\ Y_1 &= 1.562 \angle 90^\circ \text{ mS} \end{aligned} \quad (17)$$

Computing the A factor using these circuit parameters gives the following:

$$A = 0.916 \angle 0.254^\circ \quad (18)$$

Thus, for the given model with the receiving end open-circuited, the receiving-end voltage is expected to be $1/0.916 = 1.092$, or approximately 9.2 percent higher than the sending-end voltage. As the voltage level of the transmission line increases, insulation degrades faster and surge arrestors bleed off a steady-state current, reducing their useful life.

In order to maintain a level voltage profile, the shunt reactors are switched in during times of light load. Adding shunt reactors at both ends of the transmission line in the test system has the following effect on the circuit constants of the transmission line:

$$\begin{bmatrix} V_S \\ I_S \end{bmatrix} = \begin{bmatrix} 1 & 0 \\ Y_{S_reac} & 1 \end{bmatrix} \begin{bmatrix} A & B \\ C & D \end{bmatrix} \begin{bmatrix} 1 & 0 \\ Y_{R_reac} & 1 \end{bmatrix} \begin{bmatrix} V_R \\ I_R \end{bmatrix} \quad (19)$$

where:

Y_{S_reac} is the sending-end reactor admittance.

Y_{R_reac} is the receiving-end reactor admittance.

Performing the matrix multiplication, we find the following for the sending-end voltage:

$$V_S = (A + B \cdot Y_{R_reac}) \cdot V_R + B \cdot I_R \quad (20)$$

As before, we can compute the ratio of the receiving-end and sending-end voltages when the line is open-circuited as the inverse of the term $(A + B \cdot Y_{R_reac})$, renamed A_{eq} . The B term is simply the positive-sequence line impedance, and the line is compensated at both ends using shunt reactors having 3.4 H/phase, resulting in an inductive admittance at 60 Hz of $-j0.78$ mS. Substituting the known quantities into the expression for A_{eq} and taking the reciprocal yields a value of approximately 1, meaning that the sending-end voltage equals the receiving-end voltage. This result stems from the fact that the line reactors were sized to perfectly compensate the shunt capacitance of the transmission line.

The previous approximations of the ratio of the receiving-end voltage to the sending-end voltage are confirmed in the test system. Fig. 9 shows the compensated and uncompensated voltage profiles of the model with the receiving-end breakers open. The ratio of the receiving end to the sending-end voltage of the uncompensated line is shown to be 623 kV/572 kV, or 109 percent, as was calculated previously. Additionally, by inspection, the voltage magnitudes of the sending end and the

receiving end are equal when the line is compensated. The sending-end voltage differs between the two operating conditions because of the voltage drop across the source impedance.

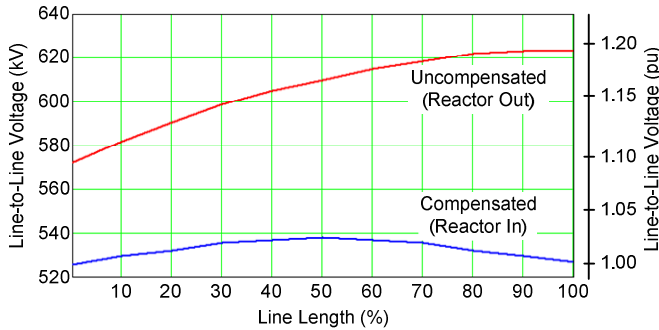


Fig. 9. Voltage profile of an unloaded line

As the line is loaded, the current in the line shifts from being predominately capacitive to more resistive in nature, the percentage of which depends upon the power factor. The resistive current flowing through the line inductance results in a voltage profile that droops in the direction of the power flow. If the shunt reactors are left in, the inductive current they draw will further exacerbate the droop of the voltage profile.

Fig. 10 shows the voltage profile along the transmission line of the test system under heavy load conditions—both with and without the shunt reactors switched in. The load current is 825 A in the simulation.

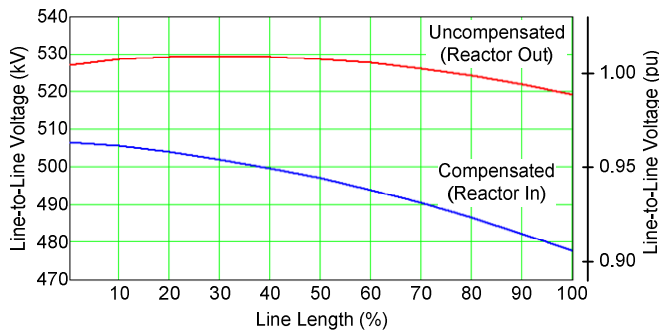


Fig. 10. Voltage profile of a loaded line

It is clear that, under heavy load conditions, the inductive current drawn by the reactor causes excessive voltage drop across the transmission line and therefore the reactors need to be switched out as the line load increases.

4) System Operation of Shunt Reactors

While the exact practices for operating shunt reactors will differ between American utilities, Oncor typically maintains its transmission-level voltages between 95 to 105 percent of the nominal operating voltage. Automated schemes are designed to monitor the line load and voltage and switch reactors in and out as necessary to keep the voltage levels within the acceptable band. Reactors are often switched out on a daily basis, sometimes multiple times each day [7]. The exact number of times that the reactors are switched in and out varies with each line and is influenced by the autotransformers in the vicinity of the line, because this also impacts the line magnitudes.

B. Faulted Power System Conditions

1) Resonance With Line Capacitance

When a single- or double-line-to-ground fault occurs and a transmission line experiences a three-pole trip, the healthy phase(s) will experience resonance between the shunt reactors and the shunt capacitance of the line.

This circuit resonance after fault clearing was demonstrated in the test system, as depicted in Fig. 11, where the A-phase experienced a fault to ground and the B-phase and C-phase resonated after the breaker tripped all three poles. Note that the B-phase and C-phase both experience an envelope superimposed on their primary resonant frequency. This envelope is a result of the circuit unbalance caused by the fault at the instant the breakers open.

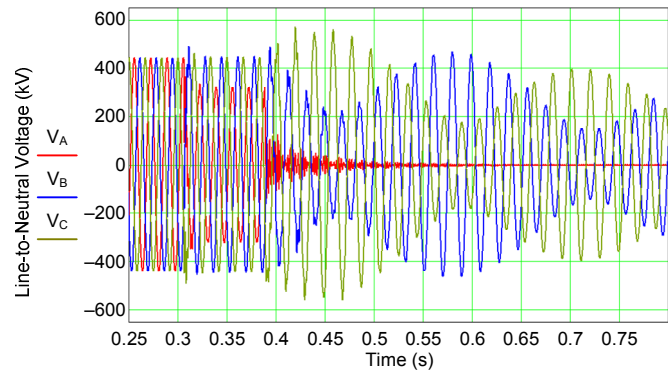


Fig. 11. Phase-to-neutral voltages of the faulted and unfaulted phases before and after the line is isolated

The frequency calculated from the three-phase voltages before and after the breaker opened (line isolated) is shown in Fig. 12. The frequency drops once the breaker opens because the shunt reactors are sized to only compensate for 80 percent of the line capacitance. This undercompensation results in a resonant frequency that is below the nominal 60 Hz of the system, typically by a few hertz.

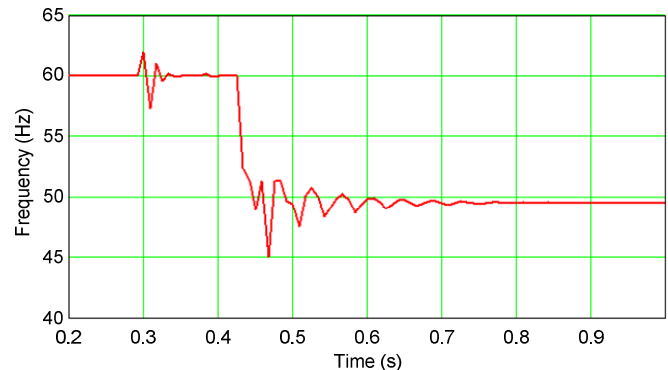


Fig. 12. Frequency of an unfaulted phase before and after the line is isolated

2) Zero-Sequence Infeed

As with any device connected to ground, shunt reactors can be a source of zero-sequence infeed during faulted or system unbalance conditions. However, because their purpose is to store energy, their zero-sequence impedance values tend to be much larger than system equivalent impedances (the zero-sequence impedance of the reactor matches the zero-sequence impedance of the line). Therefore, they draw negligible zero-

sequence current. A simple diagram of the zero-sequence circuit for the local line end during an internal single-line-to-ground fault is shown in Fig. 13. The zero-sequence current sourced through the reactor and line capacitance combination is dictated by a simple current divider.

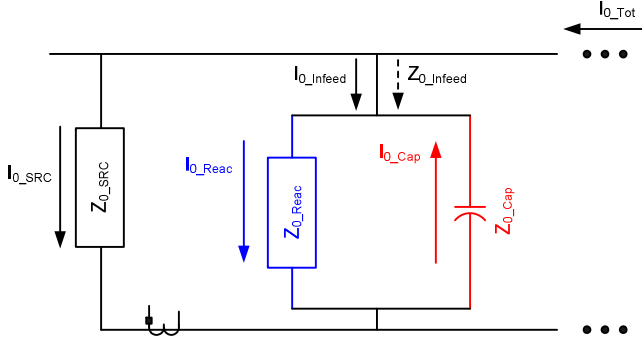


Fig. 13. Zero-sequence impedance diagram of the local end for a single-phase-to-ground fault

Solving for the ratio of the reactor/capacitor combination current to the source current (current seen by the relay) in terms of the zero-sequence impedances of the source and the reactor/capacitor gives the following:

$$\frac{I_{0_Infeed}}{I_{0_SRC}} = \frac{Z_{0_SRC}}{Z_{0_Infeed}} \quad (21)$$

where:

Z_{0_SRC} is the zero-sequence impedance of the local source.

$$Z_{0_Infeed} = \frac{j \cdot X_{0_Cap} \cdot X_{0_Reac}}{(X_{0_Cap} - X_{0_Reac})}$$

X_{0_Cap} is the zero-sequence capacitive line reactance.

X_{0_Reac} is the zero-sequence shunt reactance.

Equation (21) shows the following:

- The zero-sequence current infeed is determined by the compensation of the zero-sequence circuit (if the system is 100 percent compensated, there is no infeed effect, or $Z_{0_Infeed} = \infty$).
- The source strength determines the influence of the infeed effect; if the source is very weak, the reactor infeed may become significant.

For the test system, the ratio of the reactor neutral current to the source neutral current during a single-line-to-ground fault was 2 percent when the reactor bank included a neutral reactor and 4.3 percent when the neutral reactor was removed.

3) Switching Operations for Single-Line-to-Ground Faults

As previously mentioned, many shunt reactors are sized to undercompensate in order to remain in service under nominal load conditions. An added benefit of leaving the shunt reactors in the system is that during single-line-to-ground faults, the neutral reactor is available for secondary arc extinction, provided that the neutral reactor is properly sized according to the technique discussed in Section II. If the reactors have been switched out because of heavy load conditions and a single-

line-to-ground fault occurs on the transmission line, the protection scheme can be designed to switch the reactor bank back into service when the primary breaker has been opened, allowing for the extinction of the secondary arc. This scheme would have a level of complexity associated with it.

IV. CHALLENGES OF SHUNT REACTORS ON PROTECTION SYSTEMS

Protection schemes either include the shunt reactors within the line protection zone or exclude the shunt reactors from the line protection zone. We begin by discussing the difference between these two schemes and the protection issues unique to each scheme; we then address issues that are experienced by both schemes.

A. Including the Shunt Reactor in the Protection Zone

Fig. 14 is a sketch of the line protection zone when the line reactor is included. The line reactor may be considered as an extension of the line.

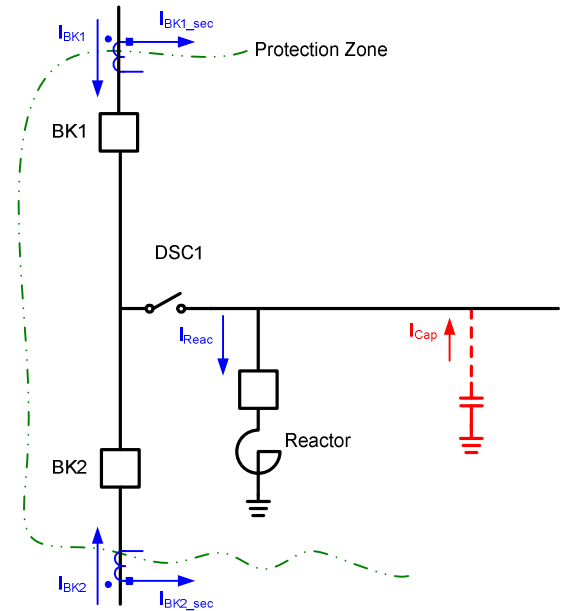


Fig. 14. Sketch of a line shunt reactor included in the line protection zone

When shunt reactors are included in the line protection zone, a fault in the reactor may result in the line protection operating and taking the line out of service. For example, a fault very close to the terminals of the reactor will have the same voltage and current profile as a fault close in to the line terminal and, as such, will be readily detected by the line protection scheme. However, a fault close to the neutral of the reactor will not be detected by the line protection scheme. Fig. 15 shows the impedance as calculated by a phase-to-ground mho distance element for a ground fault close to the neutral of the reactor on the test system.

From Fig. 15, we can clearly see that the distance element would never have detected this fault—the calculated impedance is 60 times greater than the Zone 1 reach ($Z_{1G} = 5 \Omega_{sec}$). For this reason, the reactor is equipped with its own protection scheme (e.g., a phase differential scheme).

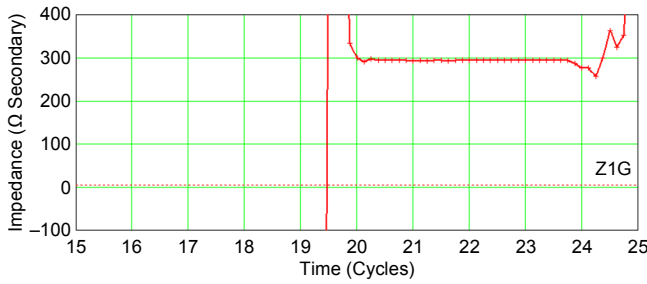


Fig. 15. Calculated impedance for a fault close to the reactor neutral terminal

Some of the reasons for leaving the reactor within the line protection zone are as follows:

- The scheme is less complex.
- The charging current compensation for the phase differential (87P) element is unnecessary.
- The line cannot be kept in service without the shunt reactor.
- The shunt reactor has its own breaker and protection scheme, and the line has the ability to autoreclose. Under these circumstances, if a fault occurs within the reactor, the dedicated reactor protection scheme will trip the reactor breaker. If the line breaker is tripped, the line breaker can be reclosed via the autoreclose function so that the line will not be permanently tripped out of service for reactor faults.

B. Excluding the Shunt Reactor From the Protection Zone

The reason why reactors are excluded from the line protection zone is so that faults in the reactor do not result in the line being taken out of service. This applies to critical lines that can function without the use of a shunt reactor. To exclude the reactors from the zone, the reactor currents must be subtracted from the current being supplied to the protection zone by the line breaker CTs. To accomplish this, the line reactors are fitted with their own CTs. This creates a protection zone as shown in Fig. 16.

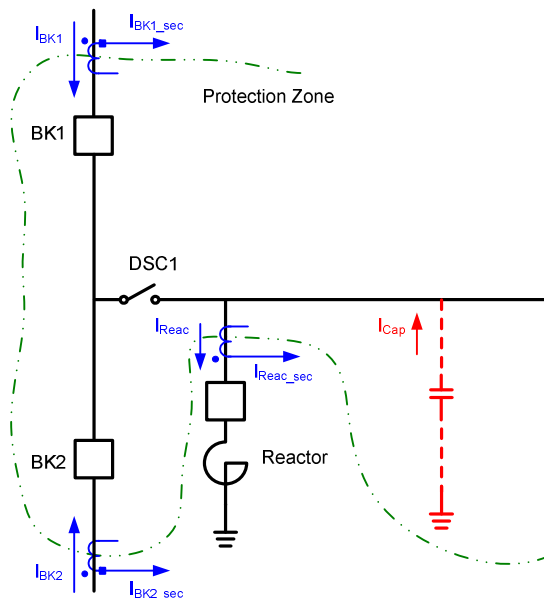


Fig. 16. Breaker and shunt reactor CT connection

The line reactor current can be subtracted from the line breaker currents in two ways. The first method is external, connecting the CTs in parallel as shown in Fig. 17.

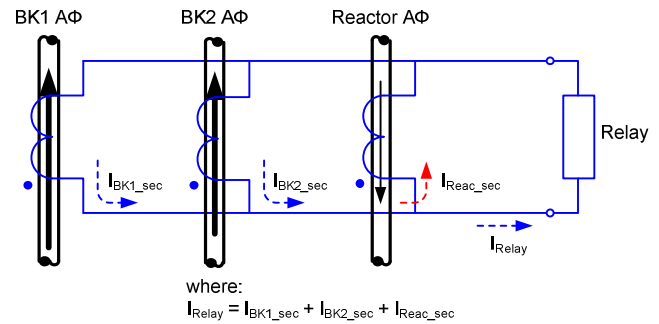


Fig. 17. Summing the currents for the protected line zone externally by connecting the CTs in parallel

The drawback of summing the CTs externally is that all the CTs must have the same ratio. If one of the CTs saturates, not only will the saturated CT not faithfully reproduce its own primary current but the healthy CTs will also circulate some of their current through the saturated CT for an internal fault, thereby further decreasing the current presented to the relay.

The second method is internal. If the line is protected by a modern digital protective relay with more than one current input, the line reactor current can be subtracted from the line breaker currents internally in the relay as follows:

$$I_{\text{Line}} = \frac{I_{\text{BK1_sec}}}{\text{TAP}_{\text{BK1}}} + \frac{I_{\text{BK2_sec}}}{\text{TAP}_{\text{BK2}}} + \frac{I_{\text{REAC_sec}}}{\text{TAP}_{\text{REAC}}} \quad (22)$$

where:

$$\text{TAP}_{\text{BK1}} = \frac{\text{CTP}_{\text{Max}}}{\text{CTP}_{\text{BK1}}}$$

$$\text{TAP}_{\text{BK2}} = \frac{\text{CTP}_{\text{Max}}}{\text{CTP}_{\text{BK2}}}$$

$$\text{TAP}_{\text{Reac}} = \frac{\text{CTP}_{\text{Max}}}{\text{CTP}_{\text{Reac}}}$$

$$\text{CTP}_{\text{Max}} = \text{Max}(\text{CTP}_{\text{BK1}}, \text{CTP}_{\text{BK2}}, \text{CTP}_{\text{Reac}})$$

CTP is the CT primary current rating.

Summing the currents internal to the relay allows the use of CTs with different ratios. Proper selection of the reactor CTs is important if the security of the scheme is to be guaranteed. We discuss this issue further in Section IV, Subsection E.

C. Charging Current Compensation

1) Steady State

In Fig. 14 and Fig. 16, we see that from the power system point of view, nothing has changed. The line reactor compensates for the line charging current, and the effective current in the line is the load current (depending on the percentage reactor compensation), as shown in Fig. 18.

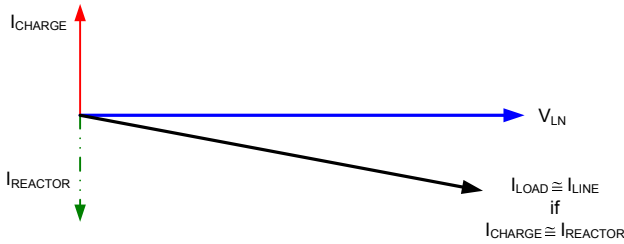


Fig. 18. Phasor diagram showing the relationship between the voltage and currents in the power system

From the protection scheme point of view, if the reactor is included in the protection zone, the current presented to the protection elements is reflective of the current in the primary system. This is not true for the protection scheme where the reactor is excluded. To see how the primary current and the current presented to the protection elements differ when the reactor is excluded, we assume the following. Breaker 1 (BK1) supplies k pu of the total current (for simplicity, we assume that the reactor and charging currents are supplied in the same ratio) in the protection zone current and Breaker 2 (BK2) the remainder:

$$\begin{aligned} I_{BK1} &= kI_{Load} + kI_{Reac} + kI_{Cap} \\ I_{BK2} &= (1-k)I_{Load} + (1-k)I_{Reac} + (1-k)I_{Cap} \end{aligned} \quad (23)$$

Substituting this into (22), we obtain:

$$\begin{aligned} I_{PROT_line} &= I_{BK1} + I_{BK2} + (-I_{Reac}) \\ &= I_{Load} + I_{Cap} \end{aligned} \quad (24)$$

From (24), we see that the protection zone contains not only the load current (I_{Load}) but also the line charging current (I_{Cap}); therefore, to agree with what is seen by the primary system current, the line charging current has to be subtracted from the protected line current. The line charging current can be calculated by multiplying the susceptance (B) of the line by the derivative of the line voltage. If we subtract the line charging current from the protection zone current (I_{PROT_line}) in (24), we obtain the load current as shown by (25).

$$\begin{aligned} I_{PROT} &= I_{PROT_line} - jB \frac{dV}{dt} \\ &= I_{Load} \end{aligned} \quad (25)$$

This is, in effect, the same as if the reactor were not removed from the protection zone. Should the line charging current not be subtracted from the protection zone current, the protection elements will be affected as follows:

- For ground distance (21G) elements, it will have a negligible effect because, under normal system conditions, the negative- and zero-sequence charging currents are negligible.
- For phase distance (21P) elements, it will result in the phase currents becoming more capacitive and moving the measured impedance towards the $-jX_C$ axis and closer towards the origin, as shown in Fig. 19.

- For ground differential (87G) elements, it will have a negligible effect for the same reason that it has no effect on the ground distance elements.
- For phase differential (87P) elements, the charging current appears as a difference current; therefore, to prevent the element from operating under steady-state conditions, the pickup current of the element will need to be increased.

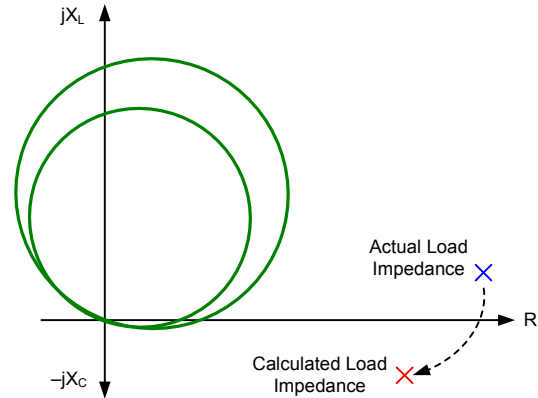


Fig. 19. Sketch showing how not compensating for the capacitive current affects the impedance calculated by a distance element

To summarize, the real charging current contributed from each end of the line is difficult to measure or calculate. For a line differential element, there is no need to know the individual contribution as long as the total charging current can be subtracted from the zone current. If the reactor is excluded from the protection zone and charging current is not subtracted from the zone current or if the shunt reactor is included in the zone but not fully compensating for the line charging current, the sensitivity of the phase differential elements must be decreased (pickup setting must be increased). The charging current, whether or not it is removed from the protection zone, has negligible impact on the performance of the distance element.

2) Transient State

In a steady state, whether the relay calculates the charging current based on voltage inputs and subtracts it from the protection zone current in real time or the charging current is counterbalanced by having the shunt reactor in the zone practically makes no difference. We now see if the same is true under the following transient conditions:

- Line energization
- In-zone fault

a) Line Energization

Fig. 20 is the circuit diagram of a section of a simple power system; by closing the breaker, the line is energized. At the instant the line is energized (breaker closes), the capacitor appears as a short circuit and the shunt reactor appears as an open circuit because of the high frequency transient. Therefore, the initial current drawn when the breaker is closed is current to charge the capacitor.

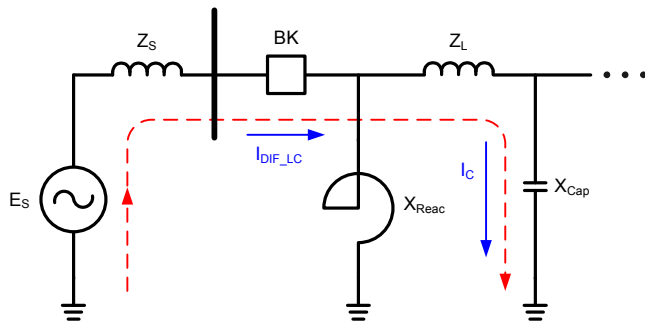


Fig. 20. Resonance between the series reactance and shunt capacitance

The magnitude of the current drawn by the capacitor is determined by the sum of the impedances of the line and the source (mainly inductive). The frequency of the current drawn is determined by the sum of the series inductances of the source and line ($L_S + L_L$) and the shunt capacitance of the line (C_L). This is known as the resonance frequency, given in hertz, and is determined as follows:

$$f = \frac{1}{2\pi\sqrt{(L_S + L_L) \cdot C_L}} \quad (26)$$

As the line capacitor becomes charged, the voltage across the capacitor increases, meaning the voltage across the shunt reactor increases. This has the following two effects:

- The current drawn by the capacitor decreases.
- The shunt reactor begins to draw current from the source.

The rate at which the capacitor is charged is known as the time constant and is determined by the sum of the source resistance and line resistance ($R_S + R_L$) and the shunt capacitance of the line (C_L).

$$\tau = (R_S + R_L) \cdot C_L \quad (27)$$

When the capacitor is fully charged, the system draws current at the nominal frequency of the power system. For the power system in the appendix, the resonance is calculated at close to 180 Hz (third-harmonic frequency). This is confirmed by a snapshot of the RTDS simulation in Fig. 21, which plots the difference between the current drawn by the shunt reactor and the shunt capacitance (I_{DIF_LC} in Fig. 20).

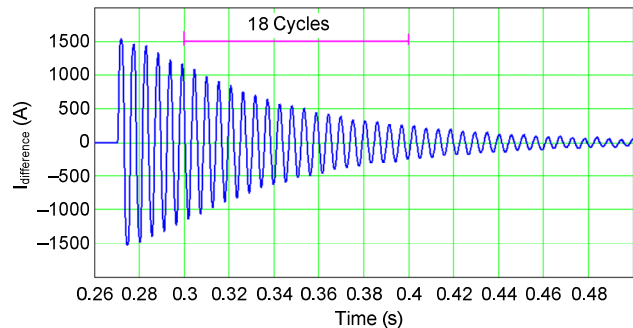


Fig. 21. Difference between the reactor and capacitor currents due to inrush

Suppose that the protection design includes the reactor in the protection zone, fully removing the charging current seen by the relay in a steady state. However, at line energization, the shunt reactor and line capacitance behave differently because of the presence of high-frequency transients, which results in transient difference currents (Fig. 21) that are detected by line differential schemes. To facilitate discussion later in this section, we define this current as I_{DIF_LC} . In summary, during the first few cycles after energization, the inductive current does not cancel the capacitive current because during the initial energization period, the line shunt capacitance is the primary current sink until the line voltage is elevated. The result is the difference current (I_{DIF_LC}) between the shunt reactor and the line shunt capacitance. This current is rich in third harmonics for our test system.

The differing behaviors of the line reactor and the line shunt capacitance during energization conditions not only challenge the scheme when the reactor is included in the protection zone but also challenge the protection scheme when the line reactor is excluded from the protection scheme and the charging current is calculated. To reduce complexity in implementation, a lumped capacitance model of the transmission line (in favor of a distributed capacitance model) is frequently used in digital relays. The transfer functions of these two models differ, with the difference being more pronounced as the line increases in length. Fig. 22 compares the charging current waveform from a digital simulation using the Bergeron model (distributed model) with the result of an instantaneous $C \cdot (dV/dt)$ calculation using the lumped model.

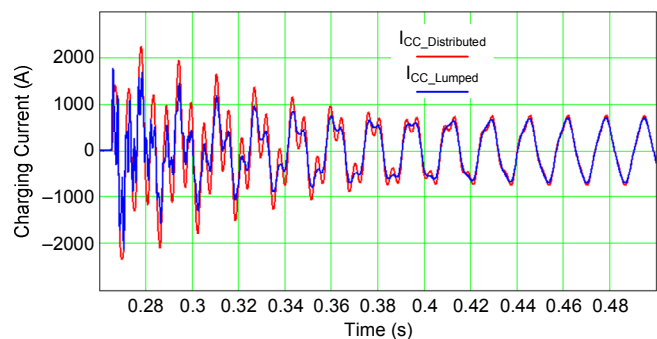


Fig. 22. Accuracy of the charging current estimation

If we examine Fig. 22, we observe that initially, the two models respond differently. However, as the high-frequency component dies out, the two models agree with one another.

The reason for the difference is that the lumped model does not correctly compensate for the higher harmonic currents. This can be proven by subtracting the charging current of the lumped model from the distributed model.

$$I_{DIF_CALC} = I_{CC_Distributed} - I_{CC_Lumped} \quad (28)$$

The result, I_{DIF_CALC} in Fig. 23, has a very similar frequency and magnitude to the difference current (I_{DIF_LC}) shown in Fig. 21.

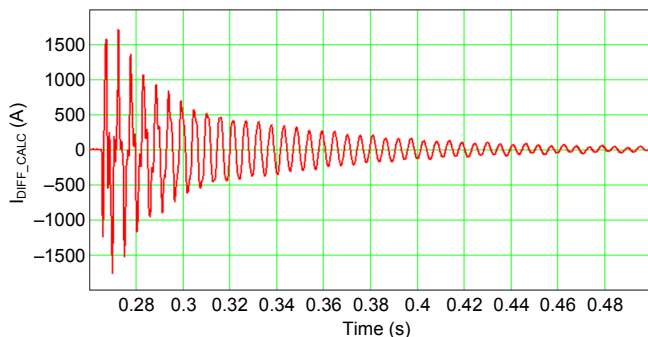


Fig. 23. Difference between the calculated (lumped) and measured (distributed) capacitance currents during line energization

Note that the difference between the distributed model and the lumped model appears as a differential current in the 87LP element. Most digital relays operate on fundamental quantities only (a finite impulse response [FIR] filter is used to remove all other harmonic frequencies); therefore, our focus is on the fundamental component of the differential current. Fig. 24 plots the magnitude of fundamental quantities with respect to time.

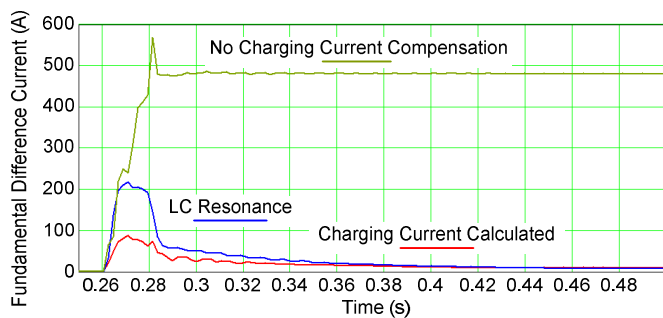


Fig. 24. Fundamental component of difference currents

The green line represents the differential current when the reactor is taken out of the protection zone and the relay does not perform charging current compensation for the differential (87L) element. The blue line represents the differential current when the line reactor is inside the protection zone. The red line represents the differential current when the reactor is taken out of the protection zone and the charging current is compensated for in the 87L elements. From Fig. 24, we see that the fundamental component (60 Hz) of the difference current between the reactor and the line shunt capacitance is lower than the root-mean-square (rms) current shown in Fig. 21, where the primary current of $1,500 A_{peak}$ translates to a secondary current of roughly $4.4 A_{rms}$. We can also see that by calculating the charging current and then subtracting it from the protection zone current (Option 1, red line), a better

dynamic response is obtained than if the reactor is within the protection zone (Option 2, blue line). However, in both instances, the difference current is less than 20 percent of the full-load current of the line CT (1200/5). This difference would not cause a misoperation of either the distance (21P) or phase differential (87P) elements. Still, the first option is more secure than the second option during single-end feed transients such as capacitive inrush. The rich harmonic content of the differential current justifies the idea of using these currents to boost the fundamental restraint of the 87L element. This way, the sensitivity of the element does not need to be compromised.

Typically, the reactor only compensates for 70 to 80 percent of the charging current. It is possible to calculate the line charging current and only subtract the portion of the charging current not compensated by the reactor from the current entering the protection zone (compensated for net capacitance). This is usually not done because more sensitive 87L settings can be applied by letting the relay compensate for full line charging current because the relay needs to run such a calculation anyway.

b) In-Zone Faults

We know that the charging current drawn by a transmission line is dependent on the susceptance (jB) of the line and the voltage of the line. During a fault condition, the line susceptance does not change but the voltage magnitude along the line decreases, as shown by Fig. 25.

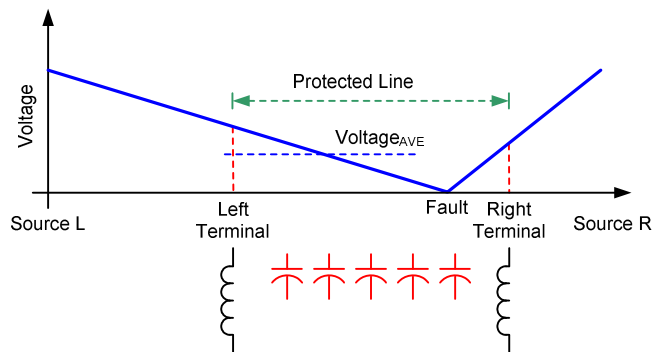


Fig. 25. System voltage magnitude profile for an in-line fault

A decrease of the line voltage results in not only the line charging current decreasing but also the compensation current from the reactor decreasing. Therefore, when the reactor is included in the protection scheme, the reactor current and line charging current magnitudes change in a similar way. However, the reactors are connected to the terminals of the line where, for an in-line fault, the voltages will be higher than any other location of the line. The capacitive current drawn by the line is determined by the susceptance (B) of the line and the average line voltage. Because the average voltage of the line ($Voltage_{AVE}$) for an in-line fault will be lower than the terminal voltage, the charging current for the line will be lower. The result is that during an in-line fault condition, the reactor current decrease is lower than the charging current decrease. Because the reactor typically only compensates for 70 to 80 percent of the charging current, the difference becomes less significant under these in-line fault conditions.

When the reactor is excluded from the protection zone, the reactor current will also decrease because of the decrease in the line voltage. If the charging current is calculated using the measured line voltage, this is a self-regulating process because the charging current calculated by the relay will be greater than the actual charging current (the relay will use the line terminal voltage to calculate the charging current of the line and not the actual average voltage of the line). Therefore, the reactor current and calculated charging current remain in the same ratio to each other as before the fault because both see the same terminal voltage. If the reactor is excluded from the protection zone and the charging current is determined by a method not involving the measured line voltage, the reactor current and charging current will not self-regulate during a fault condition. As a result, the relay will be presented a charging current greater than in the actual primary power system. It can be argued that during fault conditions for a strong system, the fault current is much larger than the charging current and, as such, this becomes a nonissue; however, this influences the accuracy of impedance-based fault location methods.

D. Reactor Ringdown

Fig. 11 is a plot of the line voltages for a fault on the test power system. As we can see, once the line is isolated, the voltages on the unfaulted phases begin to oscillate and ring down. The reason for this is explained in Section III. We can ask, “Why does this impact the protection scheme?” The line is isolated, and the fault is cleared. This is a valid argument unless the protection scheme being used is a distance protection scheme where the distance elements are polarized using memory voltage and the potential transformers (PTs) are located on the line. Under these conditions, the memory voltage logic may memorize the ringdown voltage and use this when the line is re-energized. From Fig. 12, we see that for our test system, once the line is isolated, the energy trapped in the shunt reactor and capacitor results in a voltage that has a frequency of approximately 49 Hz. To see how this impacts the memory voltage of a distance relay, we plot the voltage magnitude as calculated by a distance relay before, during, and after a fault. Fig. 26 is a plot of the voltage magnitude as calculated by a distance relay for a fault on the same test system.

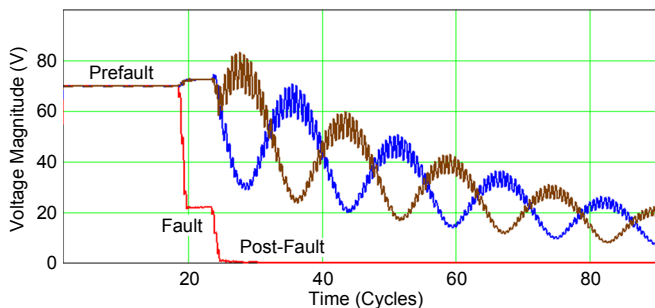


Fig. 26. Voltage magnitudes as calculated by a distance element before, during, and after a fault on the test system

From Fig. 26, we can see that during the prefault and fault time periods, the voltage magnitude calculated by the relay is consistent; however, once the line is isolated, the calculated voltage is no longer consistent but is oscillatory. The reason for this is that the relay is sampling this voltage at an integer value of 60 Hz when the system is in fact at 49 Hz, which is why the magnitude calculation is oscillating. As the relay tracks to the new frequency, the oscillation decreases and the magnitude calculation becomes more stable. The problem is that the relay memorizes the voltage at a frequency of 49 Hz and the relay uses that voltage once the line is re-energized, which can lead to a misoperation of the distance elements. To prevent such a situation, distance relays need to be equipped with ringdown detection logic to flush the memory voltage (set memory voltage to zero), so when the line is re-energized, the distance elements will be momentarily blocked (0.5 to 0.75 cycle) while the memory voltage is recharged. If a relay does not have ringdown logic to clear the memory voltage as described, then we extend the reclosing open interval delay beyond the relay memory action.

In a similar manner, for a single-pole tripping design, the voltage from the opened phase should be excluded from either frequency tracking or the memory voltage calculation. The unfaulted phases still provide voltages that can be used to update the polarization voltage so that the distance protection need not be interrupted.

E. Reactor CT Selection Criteria

It could be argued that this section is only valid for protection schemes where the reactor is excluded from the protection zone, but the data presented here are also relevant for schemes where the reactor is included in the line protection zone. We examine how both ac and dc saturation of the CTs can affect the performance of the protection scheme and what measures can be taken to secure the schemes under such conditions.

1) DC Saturation

As pointed out in Section III, when a reactor is energized, the core saturation and magnetizing inrush are not as severe as in the case of a power transformer. The concern for protective relay applications for reactors is the large X/R ratio of the reactor, which may produce a slowly decaying dc offset when the reactor is energized. This long-lasting dc component can drive the reactor CT into saturation. A well-known equation for selecting CTs to avoid saturation is [8]:

$$\left(1 + \frac{X}{R}\right) \cdot I \cdot R_b \leq ALF \quad (29)$$

where:

I is the pu current.

R_b is the pu burden resistance.

ALF is the accuracy limit factor (20 for C-class CTs).

Even though reactors draw a relatively small energization current and the CT burden for a digital relay and associated wiring is low, the X/R value of the reactor is high enough to violate the criteria in (29). Therefore, it is desirable under unfaulted system conditions for a protective relay to detect if the dc component of any current input is greater than a percentage of the ac component, as shown in Fig. 27.

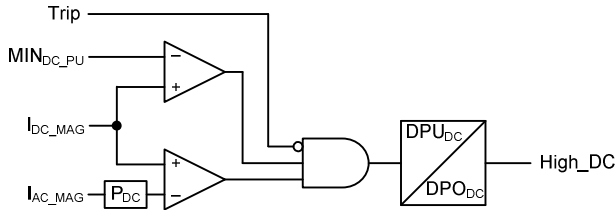


Fig. 27. DC saturation detection logic

For a distance protection (21P) scheme, CT saturation translates into an underreaching condition, so a misoperation of the distance element due to dc saturation under unfaulted system conditions is not an issue. However, the sensitivity of the scheme is compromised. One way to restore the sensitivity of the scheme is that if the current signal that experiences high dc content is from the line reactor, we can include the reactor in the protection zone and not compensate for the charging current. This method has the drawback that a fault in the reactor will result in the line being tripped.

For a differential (87L) element, CT saturation decreases the security of the scheme. Therefore, if the relay detects high dc content on any of the current inputs, the differential element should be switched into a high-security mode [9]. The following may be designed into a high-security mode:

- The pickup current setting is increased.
- The slope setting is increased.
- The security counts are increased.

In high-security mode, the 87L element is not blocked but the sensitivity of the element is decreased.

For a directional overcurrent (67Q or 67G) element, CT saturation produces secondary sequence currents that do not exist in the primary circuit. Due to the lack of sequence voltage, an impedance-based directional element with an offset characteristic may see the fault as forward. Proper security can be provided by performing the following:

- Increasing the pickup current setting.
- Increasing the positive-sequence restraint factor.

Note that either of these actions reduces the fault resistance coverage.

2) AC Saturation

Should a fault occur within the reactor zone close to the terminals of the reactor (Fig. 28), the fault current will be the same as for a fault directly in front of the relay—the only difference is that the reactor CT will see much more current than either of the breaker CTs.

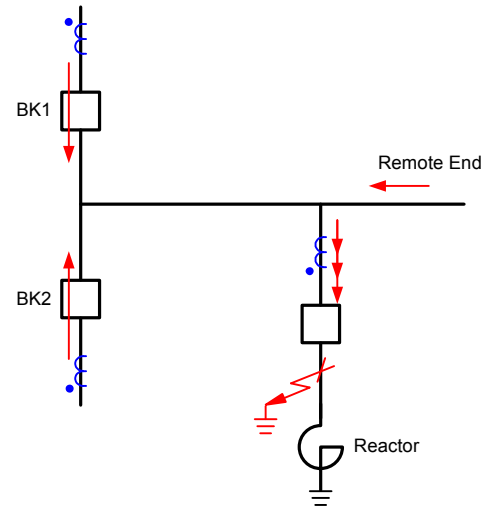


Fig. 28. External fault at reactor terminal

This means that the possibility of the reactor CT saturating is very high. When selecting a reactor CT, it may not be possible to select a CT that meets the criteria given by (29). If this is the case, ensure that the following are met.

a) Distance Element

The reverse directional elements can assert before the CT saturates (typically 0.75 to 1 cycle). Directional elements have a high tolerance for CT saturation.

b) Differential Element

For this element, it is suggested that the relay be equipped with external fault detection logic. This logic secures the differential element in the presence of high-magnitude ac fault currents. The logic requires that the CT faithfully reproduce the primary current for 0.25 cycle. The external fault detection logic in Fig. 29 measures the change in the difference current (I_{DIF}) and restraint current (I_{RST}). If the logic detects a change in the restraint current without a corresponding change in the difference current for 0.25 cycle, the logic declares the fault as external.

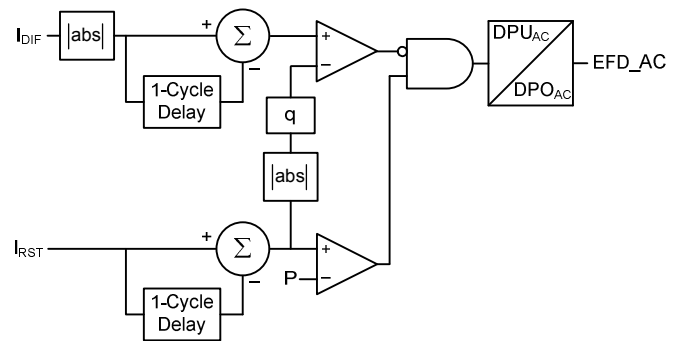


Fig. 29. External fault detection logic

Similar to the dc saturation logic when the relay detects the fault as being external, the differential element is switched into high-security mode.

F. Breaker Failure Consideration

If the line protection device has enough current inputs to facilitate each individual CT that bounds the line zone at one terminal, then the line protection device can provide individual breaker failure protection for each breaker.

Should the protection device not have enough current inputs to individually facilitate each CT that bounds the protection zone and two or more CTs are paralleled externally before being input to the protection device, then the line protection device should not be called upon to facilitate breaker failure protection. This is because the line relay will not be able to distinguish which current is associated with which breaker. In this case, breaker failure protection should be performed by a separate device on a per-breaker basis.

V. CONCLUSION

Shunt reactors are used in power systems to counteract the effect of the line parasitic capacitance, thereby stabilizing the system voltage within acceptable limits. The greatest threat posed by shunt reactors to sensitive line protection (67Q, 67G, 87LQ, and 87LG) schemes is when they are energized or they experience faults close to their terminals if the reactor is excluded from the protection zone. For these situations, it is recommended that the protection scheme be secured by dc saturation and external fault detection logic.

Infeed from the shunt reactor during faults on the power system is not a concern because the percentage of fault current contributed by the shunt reactor is negligible and, for all practical purposes, can be neglected.

Distance relays that are memory voltage polarized and are connected to the power system via line PTs need to be fitted with ringdown detection so as not to corrupt the memory voltage when the line is de-energized.

When applying sensitive protection elements, excluding the reactor from the line protection zone requires the protection device to compensate for the line charging current, whereas if the reactor is included in the zone of protection, this is not strictly required. When considering line protection, there is not a significant advantage in including or excluding the shunt reactor from the protection zone.

VI. APPENDIX

This appendix includes the circuit diagram and details of an RTDS model power system. We used this model to validate the equations presented in this paper and to obtain the transient and steady-state waveforms that are presented.

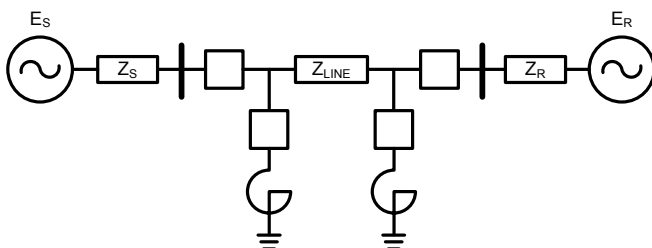


Fig. 30. RTDS model power system used

TABLE I
525 kV OVERHEAD TRANSMISSION LINE SYSTEM DATA

Parameter		Value
Rated line-to-line voltage		525 kV
Line length		200 miles
Line impedance	Z_{1L} (positive-sequence impedance)	107.68 $\Omega \angle 87.33^\circ$
	r (positive-sequence resistance)	0.0251 Ω/mile
	l (positive-sequence inductance)	1.427 mH/mile
	Z_{0L} (zero-sequence impedance)	434.48 $\Omega \angle 82.19^\circ$
	r (zero-sequence resistance)	0.2952 Ω/mile
	l (zero-sequence inductance)	5.709 mH/mile
	B_{1L} (positive-sequence capacitive shunt susceptance)	1.562 mS
	C_1 (positive-sequence capacitance)	0.02071 $\mu\text{F}/\text{mile}$
	B_{0L} (zero-sequence capacitive shunt susceptance)	0.730 mS
	C_0 (zero-sequence capacitance)	0.00969 $\mu\text{F}/\text{mile}$
Local source impedance	Z_{1S} (positive-sequence impedance)	35 $\Omega \angle 88.0^\circ$
	Z_{0S} (zero-sequence impedance)	45 $\Omega \angle 88.0^\circ$
Remote source impedance	Z_{1R} (positive-sequence impedance)	200 $\Omega \angle 83.0^\circ$
	Z_{0R} (zero-sequence impedance)	250 $\Omega \angle 83.0^\circ$
Nominal load current		800 A

VII. REFERENCES

- [1] W. D. Stevenson, Jr., *Elements of Power System Analysis*, 4th ed. McGraw-Hill, 1982.
- [2] Z. Gajić, B. Hillström, and F. Mekić, "HV Shunt Reactor Secrets for Protection Engineers," proceedings of the 30th Annual Western Protective Relay Conference, Spokane, WA, October 2003.
- [3] E. W. Kimbark, "Suppression of Ground-Fault Arcs on Single-Pole Switched EHV Lines by Shunt Reactors," *IEEE Transactions on Power Apparatus and Systems*, Vol. 83, Issue 3, pp. 285–290, March 1964.
- [4] IEEE Standard 1048-2003, IEEE Guide for Protective Grounding of Power Lines.
- [5] CIGRE WG 13.07, "Controlled Switching of HVAC Circuit Breakers: Guide for Application," Part 2, *ELECTRA*, No. 185, August 1999.
- [6] D. Goldsworthy, T. Roseburg, D. Tziouvaras, and J. Pope, "Controlled Switching of HVAC Circuit Breakers: Application Examples and Benefits," proceedings of the 34th Annual Western Protective Relay Conference, Spokane, WA, October 2007.
- [7] IEEE Standard C37.015-2009, IEEE Guide for the Application of Shunt Reactor Switching.
- [8] G. Benmouyal, J. Roberts, and S. E. Zocholl, "Selecting CTs to Optimize Relay Performance," proceedings of the 23rd Annual Western Protective Relay Conference, Spokane, WA, October 1996.
- [9] B. Kasztenny, G. Benmouyal, H. J. Altuve, and N. Fischer, "Tutorial on Operating Characteristics of Microprocessor-Based Multiterminal Line Current Differential Relays," proceedings of the 38th Annual Western Protective Relay Conference, Spokane, WA, October 2011.

VIII. BIOGRAPHIES

Eithar Nashawati is a conceptual design engineer in system protection at Oncor Electric Delivery and a Ph.D. student with the School of Electrical Engineering at the University of Texas at Arlington. He received his MSEE degree from the University of Texas at Arlington in 2004. He received his BSEE degree from the University of Damascus in 1999. He worked as a lead protection and control engineer and as an area substation engineer at Progress Energy. Mr. Nashawati is a registered professional engineer in the states of Texas and North Carolina.

Normann Fischer received a Higher Diploma in Technology, with honors, from Witwatersrand Technikon, Johannesburg in 1988, a BSEE, with honors, from the University of Cape Town in 1993, and an MSEE from the University of Idaho in 2005. He joined Eskom as a protection technician in 1984 and was a senior design engineer in the Eskom protection design department for three years. He then joined IST Energy as a senior design engineer in 1996. In 1999, he joined Schweitzer Engineering Laboratories, Inc. as a power engineer in the research and development division. Mr. Fischer is currently a member of IEEE and ASEE.

Bin Le received his BSEE from Shanghai Jiao Tong University in 2006 and an MSEE degree from the University of Texas at Austin in 2008. He has been employed by Schweitzer Engineering Laboratories, Inc. ever since. Mr. Le currently holds the position of power engineer in the research and development division.

Douglas Taylor received his BSEE and MSEE degrees from the University of Idaho in 2007 and 2009. Since 2009, he has worked at Schweitzer Engineering Laboratories, Inc. and currently is a power engineer in the transmission engineering group of the research and development division.